

# Generation of multi-color attosecond x-ray radiation through modulation compression

Ji Qiang<sup>1,a)</sup> and Juhao Wu<sup>2</sup>

<sup>1</sup>Lawrence Berkeley National Laboratory, Berkeley, California 94720, USA

<sup>2</sup>SLAC National Accelerator Laboratory, Menlo Park, California 94025, USA

(Received 26 February 2011; accepted 3 August 2011; published online 22 August 2011)

In this paper, we propose a scheme to generate tunable multi-color attosecond coherent x-ray radiation. This scheme uses a modulation compression method to generate a multi-spike prebunched kilo-ampere peak current electron beam from a few tens ampere electron beam out of a linac. Such a beam transporting through a series of undulator radiators and bunch compressors generates multi-color coherent x-ray radiation. As an illustration, we present an example to generate two attosecond pulses with 2.2 nm and 3 nm coherent x-ray radiation wavelength and more than 200 MW peak power using a 50 A 200 nm laser seeded electron beam. © 2011 American Institute of Physics. [doi:10.1063/1.3629769]

Attosecond coherent x-ray source provides an important tool to study ultra-fast dynamic process in biology, chemistry, physics, and material science. In recent years, there is growing interest in generating attosecond x-ray radiation pulse using free electron lasers.<sup>1-7</sup> Most of those schemes generate a single color attosecond pulse x-ray radiation except that in Ref. 7, where two attosecond x-ray radiation pulses with different radiation wavelengths (colors) were produced based on an echo scheme. Meanwhile, multi-color attosecond x-ray radiation has important applications in time-resolved experiments such as multidimensional x-ray spectroscopy by either exciting or probing different types of atom in a system.<sup>8</sup> In Ref. 7, the second color attosecond pulse radiation was produced using another a few-cycle laser modulator, a bunch compressor, and a short undulator radiator. In this paper, we propose a scheme to generate such tunable multi-color attosecond coherent x-ray radiation based on an improved modulation compression method.<sup>9</sup> This scheme avoids the usage of another laser modulator to produce an extra color attosecond x-radiation. It also uses a low current (~tens amperes) electron beam out of a linac instead of a kilo-ampere electron beam used in previous studies.

A schematic plot of the scheme to generate multi-color attosecond x-ray radiation is given in Fig. 1. It consists of an energy chirped electron beam, a seeding laser modulator, a bunch compressor A, a laser chirper, a bunch compressor B1, an undulator radiator one, a bunch compressor B2, another undulator radiator two, and a number of repeating bunch compressors and radiators for multi-color x-ray radiation. Here, a laser chirper is a laser modulator that is used to provide local energy chirp to an electron beam. Assume an initial beam longitudinal phase space distribution of the beam as  $f(z, \delta) = F(z, (\delta - hz)/\sigma)$ , where  $z$  is the relative longitudinal distance with respect to the reference particle,  $\delta = \Delta E/E$  is the relative energy deviation,  $h$  is the initial beam energy chirp, and  $\sigma$  is the initial uncorrelated energy spread. By properly choosing the momentum compaction factor of bunch compressor B such that

$$R_{56}^b = -R_{56}^a/M, \quad (1)$$

the longitudinal phase space distribution after the bunch compressor B1 can be written as

$$f(z, \delta) = F(Mz, [\delta - M\tilde{h}z - M\text{Asin}(kMz)]/M\sigma), \quad (2)$$

where

$$M = 1 + h_b R_{56}^a, \quad (3)$$

represents the total modulation compression factor,  $\tilde{h} = h_b/C + h$ ,  $C$  is the compression factor from the first bunch compressor A,  $h_b$  is the energy chirp introduced by the laser chirper,  $R_{56}^a$  is the momentum compaction factor of the first bunch compressor,  $A$  is the modulation amplitude of the seeding laser in the unit of the relative energy, and  $k$  is the wave number of the seeding laser. The above distribution function represents a compressed modulation in a chirped beam. In the above equations, we have also assumed a longitudinally frozen electron beam and a linear laser chirper instead of the real sinusoidal function from the laser modulator.

The linear chirp in Eq. (3) from a sinusoidal laser chirper modulation can be approximated as  $h_b = A_b k_b$ , where  $A_b$  is the amplitude of the laser modulation and  $k_b$  is the wavenumber of the laser. The sinusoidal form of the energy modulation provides periodical energy chirping/unchirping across the beam. If the amplitude envelop of the sinusoidal energy modulation is controlled externally, the periodical local chirping of the beam can be controlled. From Eq. (3), the local modulation compression factor can be controlled across the beam. This results in a periodically separated locally modulated beam with different modulation wavelengths. For a Gaussian laser beam, the energy modulation caused by the laser chirper is assumed as

$$\delta = \delta + A_b \sin(k_b z) \exp\left(-\frac{1}{2} \frac{z^2}{\sigma_b^2}\right), \quad (4)$$

<sup>a)</sup>Electronic mail: jqiang@lbl.gov.

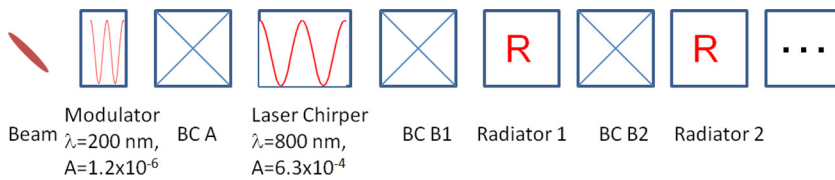


FIG. 1. (Color online) A schematic plot of the lattice layout of the modulation compression scheme.

where  $\sigma_b$  is the rms laser pulse length. The local linear chirp resulted from such a laser chirper at different wavelength separations will be

$$h_b(n\lambda) = A_b k_b \exp\left(-\frac{1}{2} \frac{(n\lambda)^2}{\sigma_b^2}\right), \quad (5)$$

where  $n = 0, \pm 1, \pm 2, \dots$ . Using Eq. (3), the resultant modulation compression factor  $M$  becomes

$$M(n\lambda) = 1 + A_b k_b \exp\left(-\frac{1}{2} \frac{(n\lambda)^2}{\sigma_b^2}\right) R_{56}^a. \quad (6)$$

From the above equation, we see that on either side of the Gaussian laser pulse (i.e.,  $n \geq 0$  or  $n \leq 0$ ), the compressed modulation wavelength will decrease with the increase of the separation. To achieve the final modulation compression, the  $R_{56}^b$  of the bunch compressor Bs after the laser chirper needs to match the condition Eq. (1). For the first local chirp  $h_b(0)$ , this can be done by using the bunch compressor B1. After the beam passes through the first radiator to generate first color radiation, the second bunch compressor B2 can be used to produce locally prebunched beam corresponding to the local chirp  $h_b(\lambda)$ . Such a locally prebunched beam passing through the second radiator will generate another color x-ray. Following the same procedure, multi-color x-ray radiation can be generated by using multiple bunch compressor and radiator pairs for different local chirp  $h_b$  and modulation compression factor.

As an illustration of the above scheme, we will produce two-color attosecond coherent x-ray radiation using a similar example in Ref. 7. A short uniform electron bunch (100  $\mu\text{m}$ ) with 17 pC charge, 2 GeV energy,  $-54.45 \text{ m}^{-1}$  energy-bunch length chirp, and an uncorrelated energy spread of  $1 \times 10^{-6}$  is assumed at the beginning of the seeding laser modulator of 200 nm wavelength. The initial normalized modulation amplitude  $A$  is  $1.2 \times 10^{-6}$ . Assuming 1 T magnetic field in the wiggler with a total length of 33 cm and a period of 11 cm, this corresponds to about 130 kW laser power. After the modulator, we add an uncorrelated energy spread of 0.56 keV to the beam to account for the synchrotron radiation effects inside the wiggler magnet. After the initial seeding laser modulator, the beam passes through the chicane bunch compressor A. Here, we have assumed that the  $R_{56}$  of the chicane is 1.763 cm. This gives a factor of 25 compression from this bunch compressor. Another 0.63 keV uncorrelated energy spread is added to the beam to account for the uncorrelated energy spread growth from the quantum fluctuation of the incoherent synchrotron radiation through the chicane. After the beam passes through the chicane, it then transports through a short-pulse laser chirper with a 800 nm resonance wavelength. Here, we assume that the energy modulation from the laser chirper follows a Gaussian en-

velop function as given in Eq. (4) with the rms laser pulse length  $\sigma_b = 1.307\lambda_b$ . The normalized amplitude of the laser for the first local chirp is chosen to be  $6.29 \times 10^{-4}$  so that the total modulation compression factor is about 88.1. This modulation amplitude corresponds to about 38 GW laser power using a single wiggler period with 0.715 T magnetic field and 22.4 cm period length. After the beam transports through the laser chirper, it passes through a dog-leg type bunch compressor B1 that can provide opposite sign  $R_{56}^b$  compared to the chicane. For a total compression factor of 88.1 of the first local chirp, the  $R_{56}^b$  for the bunch compressor B1 is about  $-0.2 \text{ mm}$ . Figure 2 shows the projected current profiles at the end of the bunch compressor B1. Here, only half of the laser pulse is used to unchirp the initial seeded beam in order to avoid the two locally prebunched attosecond beam with the same modulation wavelength due to the symmetry of the laser Gaussian envelope function. Given an initial 51 A beam current, the prebunched current inside the first spike with about 2.2 nm wavelength modulation reaches about 4.5 kA. The width of the prebunched beam is about 200 as. This is set by the half wavelength of the laser chirper and the compression of the beam. There are other lower current spikes besides the first spike separated by laser chirper wavelength inside the beam. Those spikes will not contribute significantly to the 2.2 nm attosecond radiation, since density microbunching in those spikes is very small due to the lower modulation compression factor and the mismatch of the  $R_{56}$  of the bunch compressor B1 at those spike locations.

The above highly prebunched beam passing through a short undulator R1 will generate coherent attosecond x-ray radiation. Here, we have used the GENESIS simulation code<sup>10</sup> to calculate the coherent x-ray radiation through the short undulator radiator. The normalized emittance of the electron beam is chosen to be 0.2  $\mu\text{m}$ . The length of the radiator is about 1.0 m with an undulator period of 3.33 cm. The

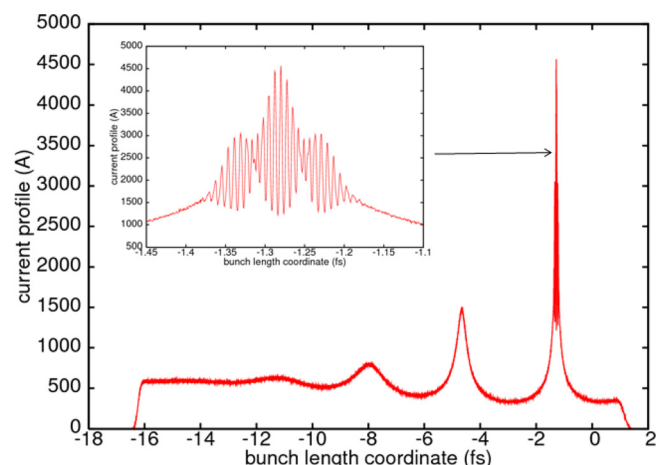


FIG. 2. (Color online) Beam current distribution at the end of the bunch compressor B1.

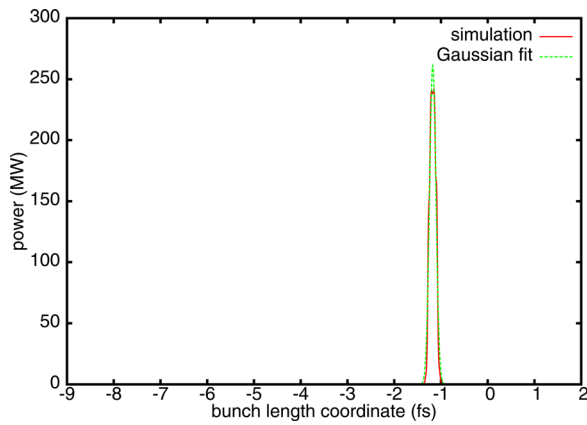


FIG. 3. (Color online) The radiation pulse temporal profile at the end of the undulator radiator 1.

radiation pulse temporal profile at the end of the radiator R1 is shown in Fig. 3. The full width at half maximum of the radiation pulse is about 200 as. The peak radiation power is about 240 MW. The time-bandwidth product of the radiation is about 0.63 that is close to the transform limit.

After the electron beam passes through the radiator R1, the output longitudinal particle distribution from the previous GENESIS simulation is used to pass through the bunch compressor B2. The  $R_{56}$  of this bunch compressor is chosen to be about  $-61.7 \mu\text{m}$  so that the modulation compression condition Eq. (1) can be satisfied for the second current spike inside the beam. This results in a modulation compression factor of about 66.0 inside that local spike. Figure 4 shows the current profile inside the second current spike of the beam at the end of the bunch compressor B2. It is seen that after this bunch compressor, the beam is significantly modulated with a wavelength about 3 nm inside the second spike. The peak current inside this spike is about 4 kA with a modulation width of about 200 as. Figure 5 shows the radiation pulse power temporal profile at the end of the radiator R2.

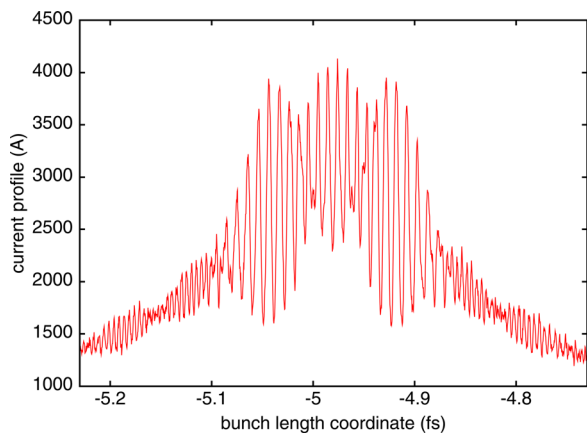


FIG. 4. (Color online) Beam current profile of the second spike at the end of the bunch compressor B2.

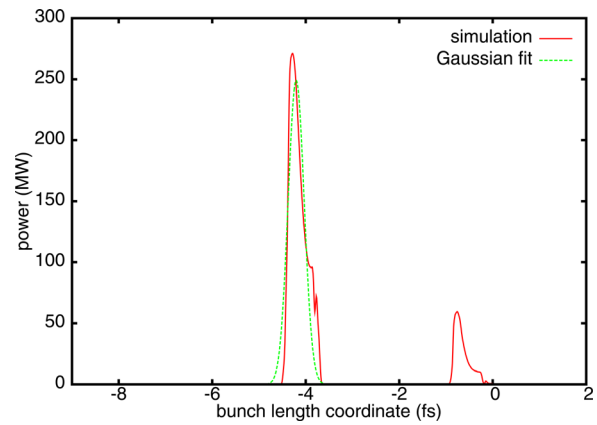


FIG. 5. (Color online) The radiation pulse temporal profile at the end of the undulator radiator 2.

Here, we have assumed that the radiator is 3.115 m long with an undulator period of 4.45 cm. The full width at half maximum of the radiation pulse is about 330 as with a radiation peak power more than 270 MW. The radiation pulse length is longer than the width of the modulated current density distribution. This is due to the slippage of the photon pulse with respect to the electron bunch inside the radiator. The radiation time-bandwidth product is about 0.85 that is also close to the transform limit. The small bump in the radiation temporal profile is due to the self-amplified spontaneous emission from the first current spike of the beam.

There are several practical effects such as the time jitter between the electron beam and the laser beam and the amplitude jitter of the laser modulation that are not included in this study. Those effects will be addressed in our future study and hopefully can be solved with the fast advances of the instrumentation and the laser technology.

We would like to thank Dr. J. Corlett, Dr. J. Wurtele, and Dr. A. Zholents for helpful discussions. This research used computer resources at the National Energy Research Scientific Computing Center. This work was supported by the U.S. Department of Energy under Contract Nos. DE-AC02-05CH11231 and DE-AC02-76SF00515.

- <sup>1</sup>A. A. Zholents and W. M. Fawley, *Phys. Rev. Lett.* **92**, 224801 (2004).
- <sup>2</sup>A. A. Zholents and G. Penn, *Phys. Rev. ST Accel. Beams* **8**, 050704 (2005).
- <sup>3</sup>E. L. Saldin, E. A. Schneidmiller, and M. V. Yurkov, *Phys. Rev. ST Accel. Beams* **9**, 050702 (2006).
- <sup>4</sup>J. Wu, P. R. Bolton, J. B. Murphy, and K. Wang, *Opt. Express* **15**, 12749 (2007).
- <sup>5</sup>Y. Ding, Z. Huang, D. Ratner, P. Bucksbaum, and H. Merdji, *Phys. Rev. ST Accel. Beams* **12**, 060703 (2009).
- <sup>6</sup>D. Xiang, Z. Huang, and G. Stupakov, *Phys. Rev. ST Accel. Beams* **12**, 060701 (2009).
- <sup>7</sup>A. A. Zholents and G. Penn, *Nucl. Instrum. Methods Phys. Res. A* **612**, 254 (2010).
- <sup>8</sup>S. Tanaka and S. Mukamel, *Phys. Rev. Lett.* **89**, 043001 (2002).
- <sup>9</sup>J. Qiang and J. Wu, *Nucl. Instrum. Methods Phys. Res. A* **640**, 228 (2011).
- <sup>10</sup>S. Reiche, *Nucl. Instrum. Methods Phys. Res. A* **429**, 243 (1999).